Ann. For. Res. 65(1): 10262-10274, 2022
ISSN: 18448135, 20652445

ANNALS OF FOREST RESEARCH
https://www.e-afr.org/

FABRICATION AND EFFECT OF THE GOLD NANOPARTICLE BY A CHEMICAL METHOD ON MEDICAL PHYSICS APPLICATIONS

Abeer Hatem Fezaa[1], Abduallah M. Ali[1], Raad M.S.Al-Haddad[2]
[1]Department of physics ,college of education for pure science, University of tikrit ,Iraq
[2]Department of physics ,college of science ,university of Baghdad ,Iraq
Corresponding Authors: Abeer Hatem Fezaa email ; abeerhatam20@gmail.com

ABSTRACT
Gold nanoparticles (AuNPs) were chemically synthesised. Their surface plasmon resonance is shifted chemically to the near-infrared spectrum. The structure of the synthesised AuNPs was examined using X-ray diffraction, transmission electron microscopy (TEM), and ultraviolet-visible spectroscopy, and they were evaluated using their zeta potential. Reducing agents were used to create the AuNP solution. The diffraction lines at 38.2°, 44.4°, 64.5°, and 77.6° correspond to the (111), (200), (220), and (311) crystal planes in their XRD patterns. As the ratio increased, the lines' width shrank, suggesting that their crystallite size had increased. The TEM image was used to assess the synthesised AuNP's size and shape, which had an average diameter of 14.73 nm and a stability of −27.1 mV. The AuNP's antibacterial activity against *Proteus mirabilis* and *Streptococcus mutans* was assessed at four dilutions (12.5%, 25%, 50%, and 100%), showing broad inhibition zones (16, 18, 21, and 23 mm) and (12, 16, 18, and 21 mm), respectively; note that the control well diameter was 6 mm AuNPs were also more effective against breast cancer cell, showing a significant cell-killing effect on them at 100 µg/mL, with a cell survival rate of 48.74%. Importantly, this concentration was below the killing threshold for normal breast cells.
Keywords: nanoparticles , antibacterial, inhibition zones, breast Cancer cells.

1. Introduction
The typical size range of nanoscale material structures is 1–100 nanometers (nm), comparable to the size of large biological molecules (e.g., enzymes and receptors). The particular interactions that nanoparticles (NPs) can have with biomolecules make them potentially helpful in diagnosis and treatment [1]. The medical potential of nanotechnology has captured the attention of most scientists. The application of gold (Au) NPs (AuNPs) for cancer detection is one intriguing area [2]. AuNPs have major potential biomedical applications (e.g., as antibodies and other biomarkers) due to their relative chemical stability (making them less dangerous), easy and straightforward synthesis and production, biocompatibility, and noninterference with other labelled biomaterials [3-5].
One of the largest threats to public health today is the rise of antimicrobial resistance, particularly given the decline in developing new safe antibacterial agents. Several approaches have been used to revitalise the current antibacterial chemotherapeutic alternatives [6,7]. AuNPs, with their large surface area, show relatively strong absorption qualities and are frequently used in colourimetric analysis detection and biological analysis by altering the refractive index of their surroundings.

Therefore, AuNPs with relatively high scattering capabilities are more appropriate for biomedical applications [8]. Nanotechnology currently shows promise as an emerging technique for producing novel antimicrobial medicines with expanded qualities such as effective targeting, improved pharmacokinetic profiles, and reduced toxicity [9].

New AuNP compounds have optical and electrical properties that differ from typical materials and show intriguing possibilities for use in medicine [10,11]. These features include their surface chemistry, which has many potential functions, surface plasmon resonance (SPR), and a stable nature with a high surface-area-to-volume ratio. AuNPs have the advantage of being readily synthesised into many shapes and sizes. Spherical AuNPs have important qualities such as optical properties associated with size and form, a high surface-to-volume ratio, excellent biocompatibility, and low toxicity [1,9]. When a laser beam strikes a metal surface at a specific angle and distance (often in the case of Au, silver [Ag], or spherical NPs), a phenomenon known as SPR occurs.

AuNPs are mostly used in medication and gene delivery, photothermal therapy, cancer cell targeting and treatment, and medical biosensing due to their inert nature and biocompatibility [3,12]. Spherical AuNPs in an aqueous solution show various hues (e.g., brown, orange, ruddy, and violet) with a size-dependent absorption peak between 500 and 550 nm [13]. Because it occurs from the collective oscillation of conduction electrons induced by resonant excitation by incoming photons, this absorption band is known as a surface plasmon band (Figure 1). However, it is not present for bulk materials or the tiniest NPs (<2 nm) [13] [14].

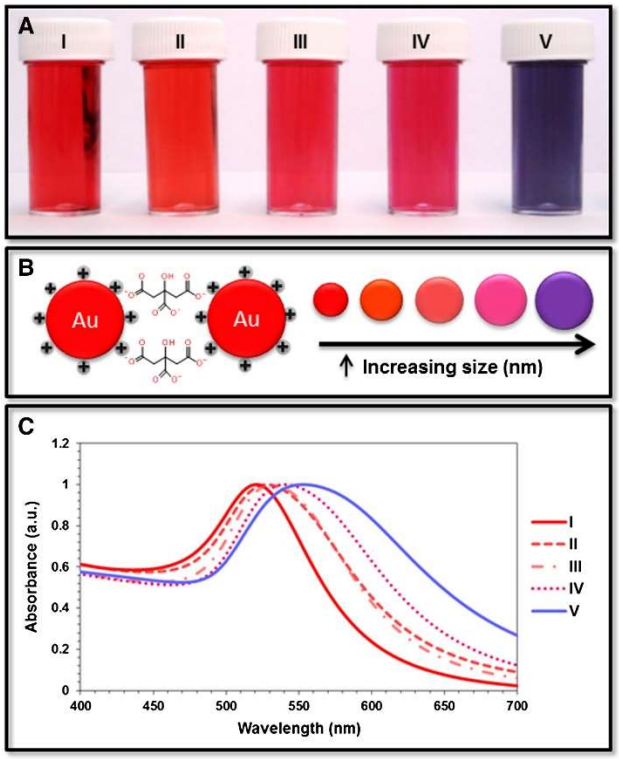

Fig. 1: A Color-changing gold solution in the preparation phases. B- different sized AuNPs with unique properties (SPR) C- each Au sol's UV-vis spectrum. [15]

AuNPs have recently generated attention in creating novel metal anticancer medicines aside from their antibacterial capabilities. In particular, AuNPs have been explored as drug transporters, contrast agents, photothermal agents, radiosensitisers, and potential cancer treatment agents. Due to their absence of immunogenicity, toxicity, and superior penetrating capabilities over standard materials, the AuNP's anticancer action is attributed to their cytotoxic effects and thiol-containing enzymes, particularly thioredoxin reductases (TrxRs), DNA damage, and mitochondrial function [9]. Furthermore, AuNPs can effectively deliver antigens to dendritic cells, enhancing cellular-mediated immune responses against cancer. Interestingly, AuNPs have also been studied for their immune-regulating and antimicrobial characteristics, enabling AuNPs to accumulate in tumours [16]. Because of their unique characteristics and diverse surface activities, AuNPs have been extensively used in bionanotechnology [17]. This study aimed to create AuNPs with antibacterial and anticancer activities via chemical synthesis for possible medicinal applications and to investigate their form, structure, and stability.

2. Experimental work:

2.1 Materials

Chloroauric acid (99%; $HAuCl_4$; molecular weight = 339.79 g/mol) was obtained from Riedel-de Hain (Seelze, Germany). Trisodium citrate dihydrate (99%; $Na_3C_6H_5O$; molecular weight = 258.07 g/mol) was obtained from PanReac AppliChem (Barcelona, Spain).

2-2AuNP's Antibacterial Activity

Gram-positive and -negative bacterial strains were used to test the AuNP's antibacterial activity in an agar-well diffusion test[18, 19] . Briefly, 20 mL of Muller–Hinton agar was aseptically poured into sterile Petri plates. Next, the bacteria were isolated from their stock cultures using a sterile wire loop [20]. Then, 6 mm diameter wells were drilled into the agar plates with a sterile point after the organisms had been cultivated. The cultivated plates with the AuNPs and test organisms were placed into the drained wells and incubated overnight at 37°C before measuring and recording the average diameter of the zones of inhibition

[21, 22].

2.3 AuNP Synthesis by the Turkevich Method

We made a 58.8 mM $HAuCl_4$ stock solution by dissolving 1 g of acid in 50 mL of deionised water. We also made a 34 mM trisodium citrate dihydrate ($Na_3C_6H_5O_7$) stock solution by dissolving 1 g in 100 mL of deionised water [23]. After heating 200 µL of the 58.8 mM $HAuCl_4$ solution on a hot plate at 75°C, 600 µL of the $Na_3C_6H_5O_7$ stock solution was added with light stirring. Figure 2 shows the colour transition from yellow to purple to ruby red. The colloidal solution was made for 1 hour and kept at room temperature.

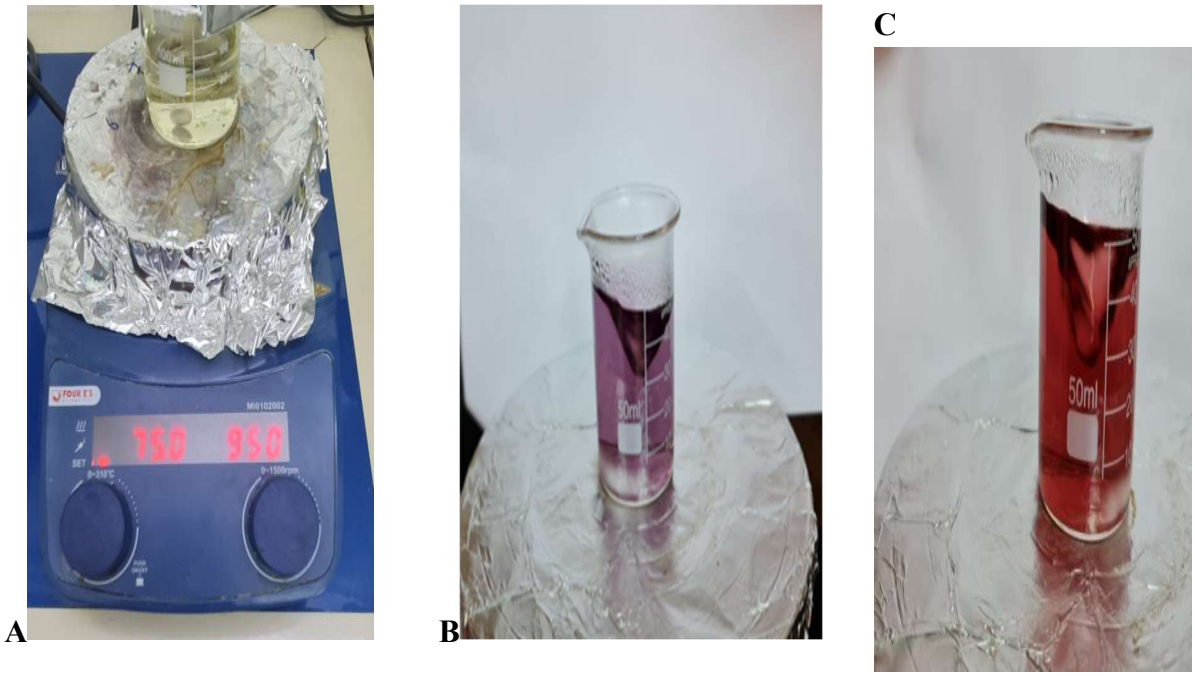

Fig. 2: Effect of solvent refractive index and heating on colour dispersion of AuNPs during preparation.

3. Results and Discussion

XRD

The X-ray diffraction (XRD) patterns of the synthesised AuNPs indicate a polycrystalline cubic Au structure, corresponding to JCPDS Card Number 96-901-3038. The diffraction peaks show that the material is nanocrystalline. Miller indices were calculated for each line to match the standard lines. The diffraction lines were present around peaks at 2θ=38.1°, 44.4°, 64.5°, and 77.6°, corresponding to the (111), (200), (220), and (311) crystal planes (hkl) They can be seen in the figure:3 and Table No.1. These findings agree with the views of Maximenko et al. [24].

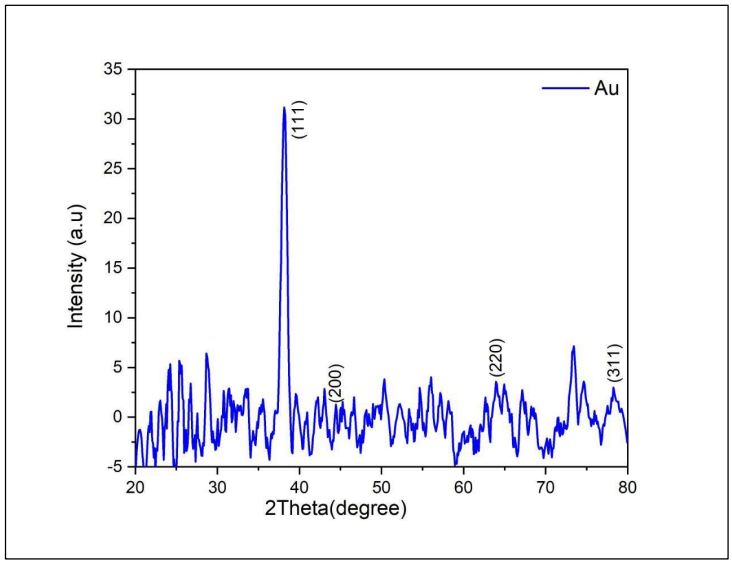

Fig. 3 AuNP XRD pattern.

Table 1: AuNP XRD characteristics.

Sample	2θ (Deg.)	FWHM* (Deg.)	d_{hkl} Exp.(Å)	**G.S (nm)	d_{hkl} Std.(Å)	hkl	$\varepsilon \times 10^{-3}$
AuNP	38.1350	0.3919	2.3580	21.4	2.3654	(111)	1.6162
	44.4146	0.7446	2.0381	11.5	2.0485	(200)	3.0079
	64.5583	0.7446	1.4424	12.6	1.4485	(220)	2.7468
	77.6094	0.7838	1.2292	13.0	1.2353	(311)	2.6651

*FWHM, full width at half maximum; **GS, graphene sponge.

UV-VIS

Ultraviolet (UV)-visible (Vis) spectroscopy was used to describe the AuNP's optical characteristics. The SPR peak for AuNPs in the 3–20 nm size range typically appears around 533 nm [25] . The pure AuNPs showed SPR peaks at 513, 515, and 521 nm for 2.5, 4 and 10 nm AuNPs, respectively (Fig. 4). The increased electron density of larger AuNPs is mostly responsible for the peak's narrowing as AuNP size increases [26 -29].

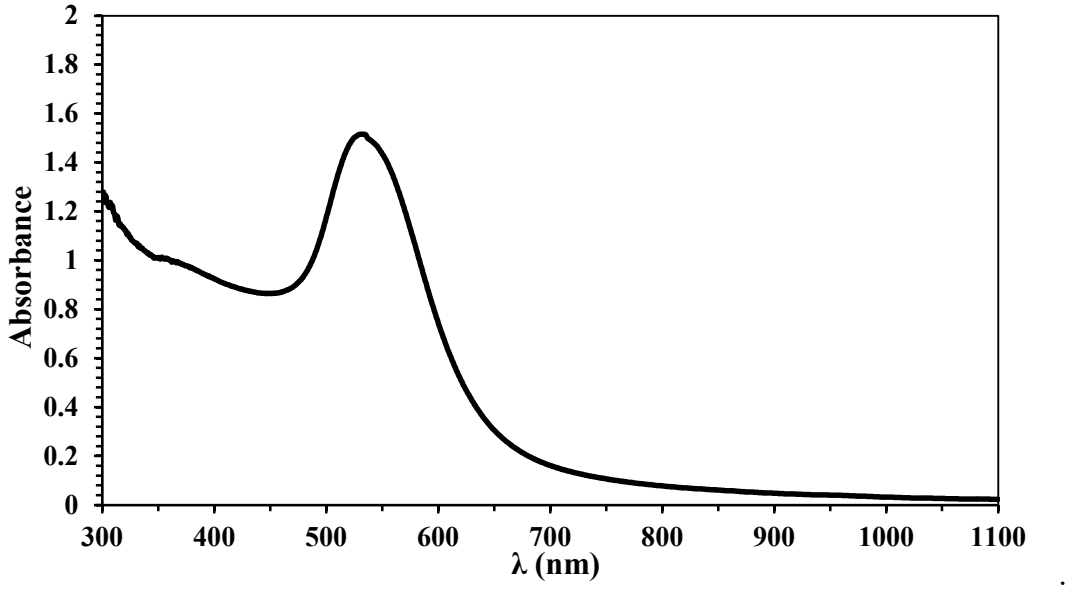

Fig. 4: **The UV-Vis spectrum of an AuNP solution.**

TEM

Transmission electron microscopy (TEM) images were used to examine the AuNP's shape and size (Fig. 5). The AuNPs had nearly uniform size and morphology and a roughly spherical shape. The produced AuNPs were mostly monodispersed, having an average diameter of 14.73 nm.

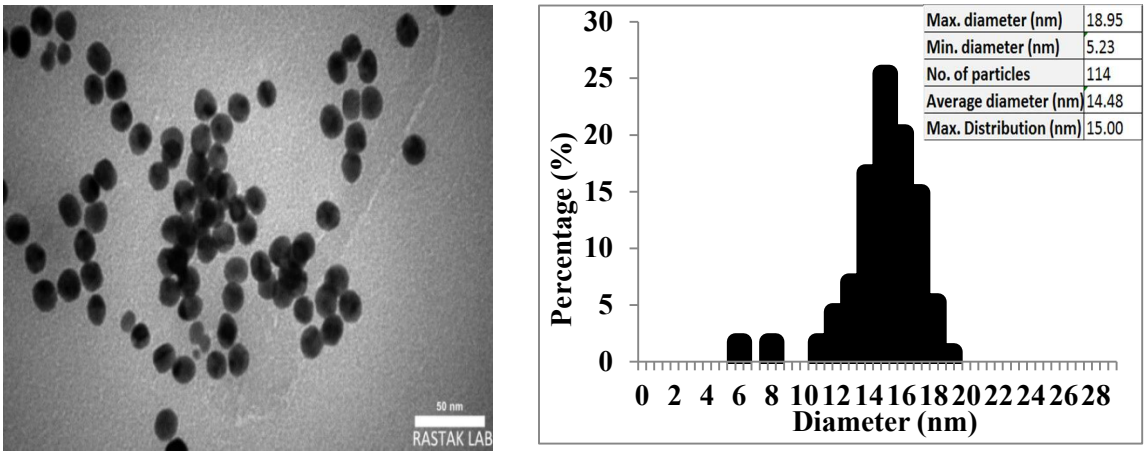

Fig. 5: A-TEM image of AuNPs. B- the size distribution of colloidal GOLD particles

Zeta potential

Zeta potential magnitude reflects the sample's stable potential sign, indicating whether positive or negative charges are more prevalent on its surface. The created AuNP's stability was evaluated using their zeta potential (Fig. 6). AuNPs with zeta potentials >+25 mV or <-25 mV are often stable. Because of their good dispersity and high suspension stability, the dispersed synthesised AuNPs in deionised water with no electrolyte had a zeta potential of -27.1 mV and are useful for medical applications.

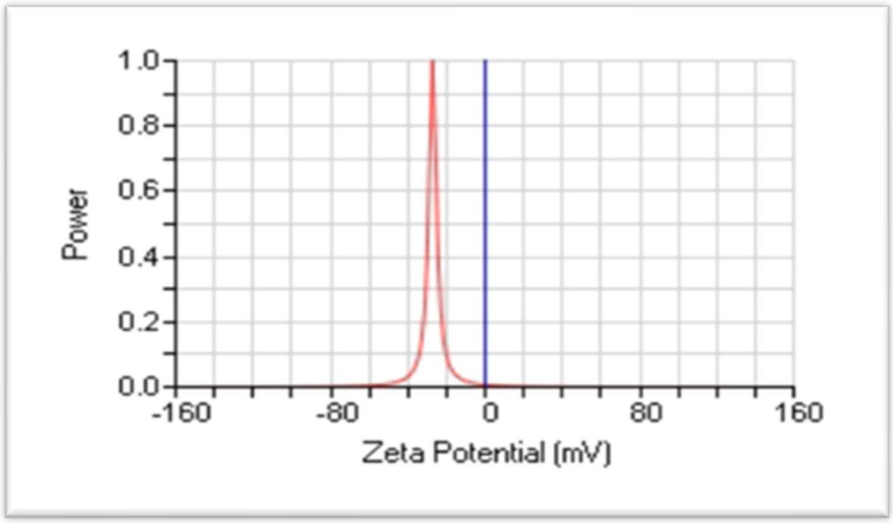

Fig. 6: AuNP zeta potential measurement.

4. Biomedical AuNP Application:

4.1. Antibacterial Activity:

Antibacterial synthetic substances, such as plant extracts or chemically modified natural compounds, limit the development of various microorganisms, including bacteria, fungi, and viruses [30,31]. The physical and chemical characteristics of materials alter when they are created as extremely tiny particles. This change in characteristics is because the surface-to-volume fraction is larger than the bulk molecule at nanoscale dimensions [32] .

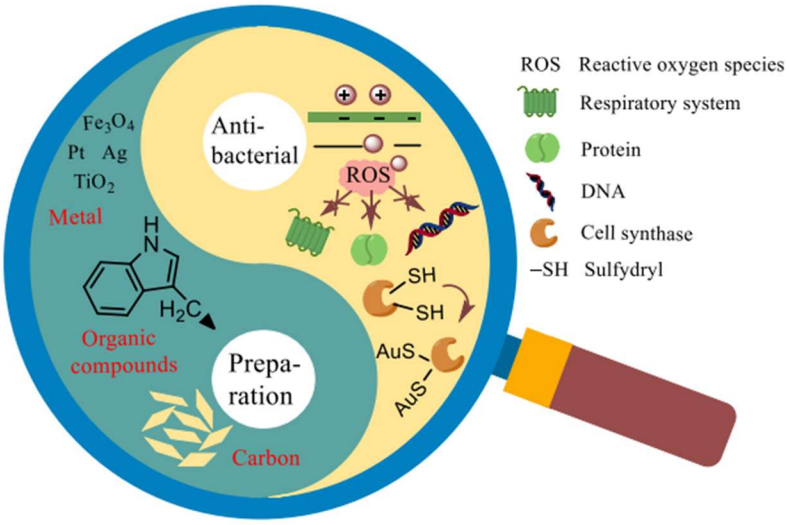

Fig. 7: An outline of the process for creating functionalised AuNPs and a description of their antibacterial qualities [33] .

4.2 Evaluation of AuNP's Antibacterial Activity

Figures 8 and 9 show the results of evaluating the AuNP's antibacterial activity using the prepared disk diffusion method against *Proteus mirabilis* and *Streptococcus mutans*, respectively. The zone of inhibition, representing reduced bacterial growth, increased with increasing AuNP concentration for *P. Mirabilis* [15,17,18,20] and *S. mutans* [12,15,17,18] relative to the control well diameter of 6 mm. The variation in bacterial microbe structure between Gram-negative and -positive strains may account for differences in the AuNP's antibacterial activity against *P. Mirabilis* and *S. mutans*. While their exterior forms differ, both bacteria have a similar core structure. Teichoic and lipoteichoic acids are found in Gram-positive bacteria's thick peptidoglycan layer. Gram-negative bacteria have a membrane comprising proteins, phospholipids, lipopolysaccharides, and a thin peptidoglycan coating. Therefore, AuNPs require a longer contact period or a greater concentration to have the same effects against *S. mutans* as against *P. mirabilis*. These results show that higher AuNP concentrations provide increased inhibition rates.

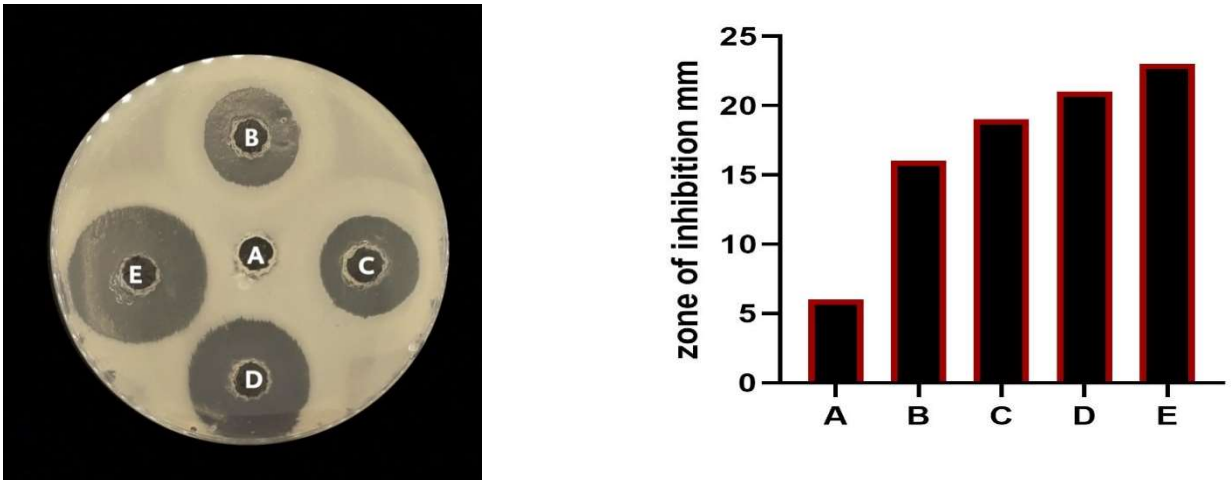

Fig. 8: Antibacterial activity of various AuNP concentrations against *P. mirabilis.* (A) Control. (B) ~12.5%. (C) ~25%. (D) ~50%. (E) ~100%.

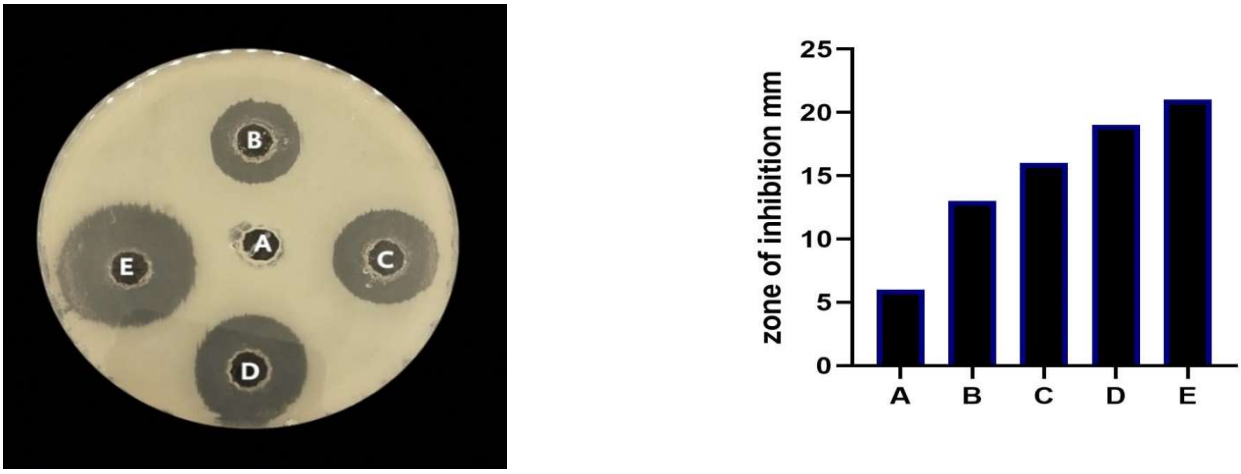

Fig. 9: Antibacterial activity of various AuNP concentrations against *S. mutans.* (A) Control. (B) ~12.5%. (C) ~25%. (D) ~50 %. (E) ~100%.

4.3 AuNP's Anticancer Activity:

Cancer is one of the leading causes of mortality globally, which has increased dramatically in recent years. Unfortunately, most established medications and methods have many adverse effects. Therefore, new medications with minimal toxicity are needed, particularly anticancer drugs produced in an environmentally friendly manner. In vitro studies have shown that AuNP's anticancer effects are dose-dependent[34–38] .They also found that the impact of a given AuNP is influenced by its shape, size, and chemistry. Smaller AuNPs appear to have a greater anticancer effect due to their higher surface area [39]. Capping agents work independently as anticancer agents while also modifying proteins or cell growth enzymes to enhance the AuNP's antiproliferative action[40–41] . The anticancer efficacy of therapeutic plant extracts is shown by their termination of cell cycle stimulation, apoptosis, and angiogenesis[42,43] . In this manner, the

adsorbed active compounds produced by plants and their medicinal efficacy with biocompatible AuNPs are crucial in cancer treatment [41] .

While the precise mechanisms through which AuNPs affect cancer cells remain unknown, the mainstays include (1) reactive oxygen species (ROS) production, (2) Cell cycle arrest, (3) glutathione (GSH) oxidation, and (4) caspases [44,45] . The AuNP's lethal impact on tumour cells is mostly a result of their great permeability of cellular barriers and affinity for diverse biological macromolecules. Through intracellular oxidative stress, AuNPs may damage cellular components and produce cytotoxicity [46, 47] . Besides protecting the cell from harmful free radicals, GSH modifies the intracellular environment's redox properties as an antioxidant. It was shown that ROS production oxidates GSH, forming glutathione disulfide [48]. The enzyme glutathione reductase, activated by oxidative stress, reduces oxidised glutathione. Therefore, increased ROS production and glutathione oxidation is the foundation of AuNP's cancer prevention.

In addition, harmful physical interactions between Au atoms and intracellular proteins' functional groups and DNA phosphate groups and nitrogenous bases contribute to AuNP's activity [49]. Cells treated with 'green' AuNPs have shown their efficiency in causing cell cycle arrest at various stages[50]. One of the most crucial mechanisms in antitumor action is inducing apoptosis, also known as programmed cell death, which can be identified morphologically via changes such as cell shrinkage, nuclear disintegration, and extensive plasma membrane blebbing [51] . Therefore, a caspase-mediated apoptotic pathway may cause cell death when AuNPs are present since most research showed morphological alterations, including cell shrinkage, nucleus disintegration, and extensive plasma membrane blebbing. Caspase-9 and Caspase-3 are activated by the B cell lymphoma-2 protein, which is essential for apoptosis and starts the apoptosis cascade. Figure (10 & 11)shows five distinct AuNP concentrations (100, 50, 25, 12.5, and 6.25 g/mL). It shows that the 100 g/mL concentration had the greatest breast cancer cell-killing effect, with a percentage of surviving cells of 48.74%. Therefore, this concentration cannot be considered lethal for killing normal cells. In contrast, the 50 g/mL concentration was nontoxic (107.6% cell proliferation occurs compared to the other concentrations), and the other concentrations had a lower percentage of surviving cells [31].

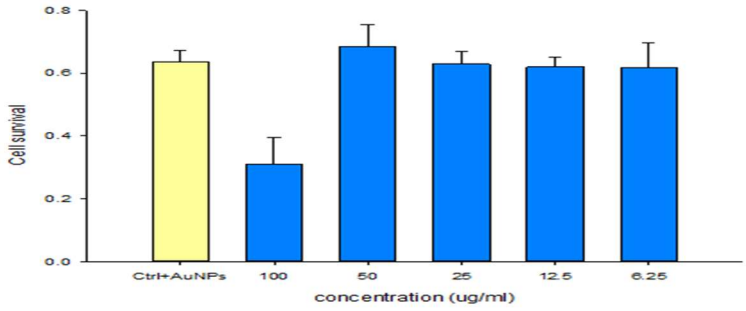

Fig. 10: Effect of different AuNP concentrations on breast cancer cells

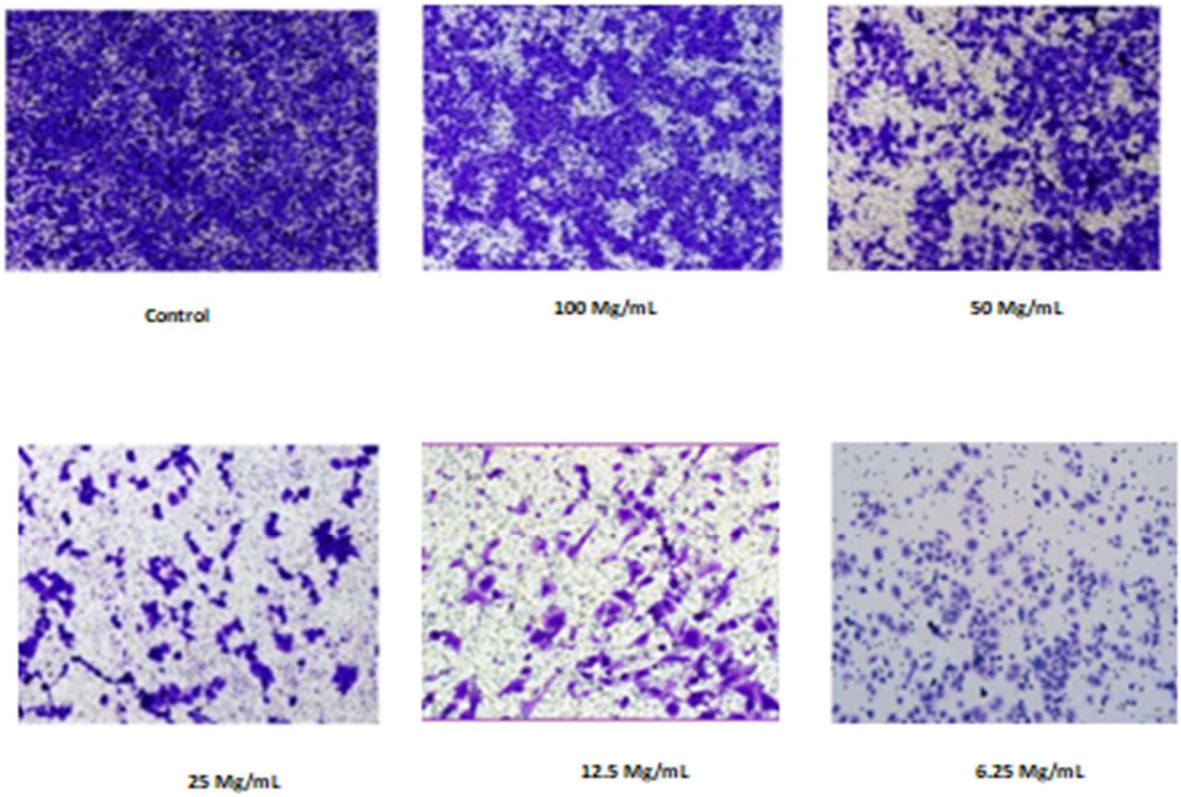

Fig. 11: Microscopy images of breast cancer cells after treatment with different AuNP concentrations (control, 100, 50, 25, 12.5, and 6.25 g.mL)

5. Conclusions

We successfully chemically synthesised AuNPs, confirmed by XRD, TEM, UV-visible, and zeta potential. This study showed that AuNP SPR is possible, showing a strong absorption band in the visible range whose energy depends on AuNP size and shape. A spherical 14.48 nm AuNP was seen in the TEM image. The absorption peak blue-shifts when AuNP size reaches a specific diameter. According to their zeta potential, the AuNPs showed a consistent dispersion of around 27.1 mV. Moreover, an AuNP concentration of 100 g/ml had a strong cell-killing effect on breast cells, with 48.74% of cells surviving.

References

[1] Zhao J., Stenzel M.H. 9, 259 (2018). doi: 10.1039/C7PY01603D

[2]Sharifi M, Avadi MR, Attar F, Dashtestani F, Ghorchian H, Rezayat SM, Saboury AA, Falahati M.126 , 773(2019). https://doi.org/10.1016/j.bios.2018.11.026

[3]Turkevich, J.; Stevenson, P.C.; Hillier, J. Discuss. Faraday Soc. (1951), *A study of* the nucleation and growth processes in the synthesis of colloidal gold.11(0),55–0. doi:10.1039/df9511100055

[4]Rawat, P.; Rajput, Y.S.; Bharti, M.K.; Sharma, R. 110, 2297(2016). doi: 10.18520/cs/v110/i12/2297-2300

[5]Okamoto,T.;Nakamura,T.;Sakota,K.;Yatsuhashi,T.35,12123(2019). https://doi.org/10.1021/acs.langmuir.9b01854
[6]Liao S, Zhang Y, Pan X, Zhu F, Jiang G, Liu Q, Cheng Z, Dai G, Wu G, Wang L, Chen L.,14:1469(2019). doi: 10.2147/IJN.S191340. e Collection 2019
[7] T. Vijay et al /International Journal of ChemTech Research, 2021,14(1): 121-129. DOI= http://dx.doi.org/10.20902/IJCTR.2021.140110
[8]ChaudharyA.;KhanS.;GuptaA.;NandiC.K. 40,4879(2016). https://doi.org/10.1039/C5NJ03720D
[9]Tao C. 67 ,537–543(2018). doi: 10.1111/lam.13082.
[10]jena M., Mishra S., Jena S., Mishra S, 2,353 (2013).doi: 10.5455/2319-2003.ijbcp20130802.
[11]WongI.Y.,BhatiaS.N.,Toner M. 27,2397 (2013). doi: 10.1101/gad.226837.113
[12] Wilton-Ely JDET. *Dalton Trans.* 2008:25–29.
[13]Boopathi S ,Senthilkumar S. ,and Phani K. L.y , 2012,6 (2011). https://doi.org/10.1155/2012/348965.
[14]P. Englebienne, A. Van Hoonacker, and M. Verhas, "Surface plasmon resonance: principles, methods and applications in biomedical sciences," *Spectroscopy*, vol. 17, no. 2-3, pp. 255– 273, 2003**.** DOI:10.1155/2003/372913
[15] NiloofarAjdari,CianVyas ,Stephanie L.Bogan ,Bashir A.Lwaleed, Brian G.Cousins"Gold nanoparticle interactions in human blood: a model evaluation"Nanomedicine: NBM, V.13, Issue 4, 2017, P. 1531-1542. https://doi.org/10.1016/j.nano.2017.01.019
[16] lmeida, J. P. M., Lin, A. Y., Figueroa, E. R., Foster, A. E., and Drezek, R. A. 11, 1453 (2015). doi:10.1002/smll.201402179
[17]Jain PK, Lee KS, El-Sayed IH, El-Sayed MA. 110, 7248(2006) .https://doi.org/10.1021/jp057170o
[18]Bahjat, H. H., Ismail, R. A., Sulaiman, G. M., and Jabir, M. S. 31, 3649 (2021). https://doi.org/10.1007/s10904-021-01973-8
[19]Khashan, K. S., Abdulameer, F. A., Jabir, M. S., Hadi, A. A., and Sulaiman, G. M. *11*, 035010(2020).. https://doi.org/10.1088/2043-6254/aba1de
[20]Khashan, K. S., Badr, B. A., Sulaiman, G. M., Jabir, M. S., and Hussain, S. A. (2021, March).Antibacterial activity of Zinc Oxide nanostructured materials synthesis by laser ablation method. In Journal of Physics: Conference Series (Vol. 1795, No. 1, p. 012040),doi:10.1088/1742-6596/1795/1/012040
[21]Jihad, M. A., Noori, F., Jabir, M. S., Albukhaty, S., AlMalki, F. A., and Alyamani,A.A. *26*,3067 (**2021)**, 3067; https://doi.org/10.3390/molecules26113067
[22]Mohammed, M. K., Mohammad, M. R., Jabir, M. S., and Ahmed, D. S. 13, 727 (2022). https://doi.org/10.47750/pnr.2022.13.03.109.
[23]G. Busch, H. Schade, Lectures on Solid State Physics: International Series in Natural Philosophy, Elsevier, 2013. DOI https://doi.org/10.1016/C2013-0-02492-9

[24]A.Maximenko, J. Depciuch, N. Łopuszyńska, M. Stec, Ż Światkowska-Warkocka, V. Bayev, P.M. Zieliński, J. Baran, J. Fedotova, W.P. Węglarz, RSC Adv. 10, 26508 (2020). https://doi.org/10.1039/D0RA03699D xrd
[25]JainL.and El-Sayed M. 110, 7238 (2006). https://doi.org/10.1021/jp057170o
[26]Bhumakar D. R., Joshi, H. M., Sastry M. and Pokharkar V. B., 2007. Chitosan reduced gold nanoparticles as novel carriers for transmucosal delivery of insulin, Pharmaceut. Res., 24(8): 1415-1426. doi: 10.1007/s11095-007-9257-9.
[27]Das R., Nath S. S. and Bhattacharjee R.,2011,1(2010). https://doi.org/10.1155/2011/630834
[28]Eustis, S., & El-Sayed, M. A. 35 ,209 (2006)..https://doi.org/10.1039/B514191E
[29]Mostafa, A. M., Mwafy, E. A., & Toghan, A. 627, 127204. (2021)https://doi.org/10.1016/j.colsurfa.
[30]Nishi, T., Takeichi, A., Azuma, H., Suzuki, N., Hioki, T., & Motohiro, T. 5, 192, (2010). DOI:10.2961/jlmn.2010.03.0002.
[31]Xiao Gu1 · Zhixiang Xu1 · Lipeng Gu1 · Huayu Xu1 · Fengxia Han1 · Bo Chen1 Xuejun Pan1,19,167(2021) https://doi.org/10.1007/s10311-020-01071-0
[32] Mikhailova, Ekaterina O. 12, 70 (2021). https://doi.org/10.3390/jfb12040070
[33] Stalin Dhas, T.; Ganesh Kumar, V.; Karthick, V.; Govindaraju, K.; Shankara Narayana, T. ,133, 102(2014). https://doi.org/10.1016/j.saa.2014.05.042
[34] Jafari, M.; Rokhbakhsh-Zamin, F.; Shakibaie, M.; Moshafie, M.H.; Ameri, A.; Rahimi,H.R.;Forootanfar,H.15, 245(2018). https://doi.org/10.1016/j.bcab.2018.06.014
[35]Stalin Dhas, T.; Ganesh Kumar, V.; Karthick, V.; Govindaraju, K.; Shankara Narayana, T., 133, 102(2014). https://doi.org/10.1016/j.saa.2014.05.042
[36]Boomi, P.; Ganesan, R.M.; Poorani, G.; Gurumallesh Prabu, H.; Ravikumare, S.; Jeyakanthan, J., 99, 202 (2019). https://doi.org/10.1016/j.msec.2019.01.105
[37]Alkilani, M.; Murphy, C.J. 12, 2313(. 2010). 10.1007/s11051-010-9911-8
[38] Jeyraj, M.; Arun, R.; Sathishkumar, G.; Mubarak Ali, D.; Rajesh, M.; Sivanandhan, G.; Kapildev, G.; Manickavasagam, M.; Thajuddin, N.; Ganapathi, A. 52, 15 (2014). https://doi.org/10.1016/j.materresbull.2013.12.060
[39]Rodríguez-León, E.; Rodríguez-Vázquez, B.E.; Martínez-Higuera, A.; Rodríguez-Beas, C.; Larios-Rodríguez, E.; Navarro, R.E.; López-Esparza, R.; Iñiguez-Palomares, R.A. 14, 334 (2019). https://doi.org/10.1186/s11671-019-3158-9.
[40] Patil, M.P.; Bayaraa, E.; Subedi, P.; Piad, L.L.A.; Tarte, N.H.; Kim, G.-D. J. Drug Deliv. Sci. Technol. 51, 83. (2019).https://doi.org/10.1016/j.jddst.2019.02.021
[41]Li, L.; Zhang, W.; Desikan Seshadri, V.D.; Cao, G. 47, 3029(2019). https://doi.org/10.1080/21691401.2019.1642902
[42]Jiao, Y.N.; Wu, L.N.; Xue, D. 18, 149(2018). https://doi.org/10.1186/s12935-018-0646-4
[43]Corbo, C.; Molinaro, R.; Parodi, A.; Furman, N.E.T.; Salvatore, F.; Tasciotti, E. 11, 81 (2016). https://doi.org/10.2217/nnm.15.188
[44]Rajathi, F.A.A.; Arumugam, R.; Saravanan, S.; Anantharaman, P. 135, 75(2014).https://doi.org/10.1016/j.jphotobiol.2014.03.016

[45] Sathishkumar, M.; Pavagadhi, S.; Mahadevan, A.; Balasubramanian, R. 114, 232(2015). https://doi.org/10.1016/j.ecoenv.2014.03.020

[46]Rajeshkumar, S., 14, 195(2016). https://doi.org/10.1016/j.jgeb.2016.05.007

[47] Ganeshkumar, M.; Sathishkumar, M.; Ponrasu, T.; Dineshc, G.M.; Suguna, L. 106, 208(2013). https://doi.org/10.1016/j.colsurfb.2013.01.035

[48]Vemuri, S.K.; Banala, R.R.; Mukherjee, S.; Uppul, P.; Gpv, S.; Gurava Reddy, A.V. Malarvilli, T. 99, 417(2019). https://doi.org/10.1016/j.msec.2019.01.123

[49]Toshiya,K.;estuya,T.;Akira,H.;Takuji,T.3,18.
https://doi.org/156201210.4236/jbpc.2012.32018

[50] Liu, X.; Kim, C.N.; Yang, J.; Jemmerson, R.; Wang, X., 86, 147(1996). https://doi.org/10.1016/S0092-8674(00)80085-9

[51] Fenglian Wu , Fenglian Wu ,Jun Zhu,Guoliang Li ,Jiaxin Wang ,Vishnu Priya Veeraraghavan and Surapaneni Krishna Mohang,(2019) , 3297-3305,Biologically synthesized green gold nanoparticles from Siberian ginseng induce growth-inhibitory effect on melanoma cells (B16),https://doi.org/10.1080/21691401.2019.1647224